NJC

Accepted Manuscript

Cite this: DOI: 10.1039/c0xx00000x

www.rsc.org/xxxxxx

PAPER

A Pyrene based schiff base probe for selective fluorescent turn-on detection of Hg^{2+} ions with live cell application

Muthaiah Shellaiah,*[a] Yesudoss Christu Rajan,[b] Perumal Balu[c] and Arumugam Murugan[a]

Received (in XXX, XXX) Xth XXXXXXXXX 20XX, Accepted Xth XXXXXXXXX 20XX

DOI: 10.1039/b000000x

A Novel pyrene based free thiol containing schiff base derivative **PT1** was synthesized via one-pot reaction and utilized as a fluorescence turn-on probe for Hg^{2+} ions detection along with live cell imaging. **PT1** in DMSO/H_2O (v/v = 7/3; pH 7.0) was showed the fluorescence turn-on response to Hg^{2+} ions, via chelation enhanced fluorescence (CHEF) through excimer **PT1-PT1*** formation. The 2:1 stoichiometry of sensor complex **PT1**+Hg^{2+} was calculated from job plot based on UV-Vis absorption titrations. In addition, the binding sites of sensor complex **PT1**+Hg^{2+} was well established from the ^{1}H NMR titrations and supported by the ESI-mass analysis and fluorescence reversibility of **PT1**+Hg^{2+} via consequent addition of Hg^{2+} ions and **EDTA**. The detection limit (LOD) and the association constant (K_a) values of **PT1**+Hg^{2+} complex were calculated by standard deviation and linear fittings and from Benesi-Hildebrand plot, respectively. Moreover, the quantum yield (Φ), time resolved photoluminescence (TRPL) decay constant (τ) changes, pH effect and density functional theory (DFT) studies were investigated for the **PT1**+Hg^{2+} sensor system. More importantly, confocal fluorescence microscopy imaging in Hela cells showed that **PT1** could be used as an effective fluorescent probe for detecting Hg^{2+} in living cells.

Introduction

Owing to the importance and toxic effect of transition metal ions on the environment, the development of selective and sensitive chemosensors for their determination has been received significant attention.[1–3] Among them, mercury is one of the most dangerous metal ions for environment because it is widely distributed in air, water and soil.[4] It can accumulate in the human body and results in wide variety of diseases even at low concentration, such as prenatal brain damage, serious cognitive and motion disorders and minamata disease.[5,6] Additionally, mercury also shows a high affinity to thiol groups in proteins and leads to the malfunction of cells and consequently leads to many diseases.[7] Therefore, the need for a highly sensitive and selective determination of mercury ions are of great consideration.

Among the available detection methods, chemosensors based on ion-induced fluorescence changes are predominantly attractive in terms of sensitivity, selectivity, response time and live cell applications.[8-10] Apart from the fluorescence quenching effects[11] of biologically important ions, recently several molecular turn-on sensors were reported for a variety of cations and anions based on photoinduced electron transfer (PET), internal charge transfer (ICT), chelation enhanced fluorescence (CHEF) and deprotonation mechanisms.[12-15] However, many of those molecules are also showed the synthetic difficulties, hence we made an attempt to develop molecules that could detect Hg^{2+} with less synthetic difficulties.[16-19]

Above considerations extend our focus in the direction of schiff bases,[20] which are recognised with simple synthetic steps, and also can applied to many cation and anion sensors. However, to develop such schiff base derivative with fluorescent turn-on sensor response towards a specific species, the presence of strong fluorophores are required.[21] In these deliberations, pyrene derivatives were demonstrated as excellent fluorophores to form dimeric structures upon the addition of certain metal cations to give P-P* excimer fluorescence with biological applications as well.[22] On the other hand, as stated before the presence of free thiol group also demonstrated its high binding affinity to Hg^{2+} ions via strong S-Hg^{2+} interactions.[23] However, many of the sulphur containing probes were also revealed the synthetic difficulties.[24] Conversely, the thiol protected probes were showed only lesser folds of fluorescence enhancement or even emission quenched with metal ions.[25, 26] Hence, we further protracted our vision in schiff base design with pyrene and free thiol containing unit by less synthetic steps and to be utilized as selective Hg^{2+} fluorescent turn-on sensor.

Herein, we synthesized a novel pyrene based free thiol containing schiff base derivative **PT1** and reported as Hg^{2+} fluorescent turn-on sensor for the first time via CHEF and excimer (**PT1-PT1***) formation with live cell imaging.

[a]Department of Chemistry, Kalasalingam University, Anand Nagar, Krishnan koil 626 190, Tamilnadu, India.
E-mail: s.muthaiah@klu.ac.in; muthaiah_s@yahoo.com
[b]Department of Food Science, Fu Jen Catholic University, Taipei, Taiwan-24205 (ROC).
[c]Department of Chemistry, Guru nanak college, Chennai 600042, Tamilnadu, India.

Table 1 Photophysical and DFT properties of **PT1** and its sensor complexes.

Composition	Tot E[a]	HOMO (eV)	LUMO (eV)	HLG[b] (eV)	λ_{abs} (nm)	λ_{em} (nm)	Φ	τ (ns)[f]
PT1	-1338.45960668	-5.3241819	-2.1347341	3.19	347	427	0.035[c] 0.041[d] 0.121[e]	2.63
PT1 + Hg^{2+}	-1940.82628043	-5.45316389	-2.97039606	2.48	365	445	0.289	3.14
PT1 + Hg^{2+} + EDTA	NA	NA	NA	NA	347	431	0.043	2.68

[a]Total Energy; [b]HOMO-LUMO Gap; Quantum yields in DMSO: H2O (9/1)[c], (7/3)[d], (5/5)[e] using 9, 10-diphenylanthracene (Φ = 0.9) as a reference standard; [f]Obtained from time resolved fluorescence measurement; NA = not applicable.

Results and Discussion

Synthesis[27] and solvent selection for sensor titrations

As shown in Scheme 1, **PT1** was synthesized via one pot pyrene-1-carboxaldehyde and 2-aminothio phenol condensation in methanol with 92% yield and characterized with ^{1}H, ^{13}C NMR and Mass (FAB) analysis (Figs. S1-S3, ESI). In order to find out the suitable solvent system for the sensor titrations, the quantum yield (Φ) calculations[28] were carried out with different mixed-aqueous media (DMSO/H_2O) as presented in Table 1. As noticed in the Table 1, from Φ value variations we found that DMSO/H_2O (v/v = 7/3; pH 7.0) was a suitable solvent system for our titrations. Hence, we performed UV/Vis/PL titrations of **PT1** (λ_{abs}=347 nm and λ_{em}=427 nm; Φ = 0.041) in DMSO/H_2O (v/v = 7/3; pH 7.0) and ^{1}H NMR titrations in [d6-DMSO] by adding metal ions in pure H_2O and D_2O, respectively.

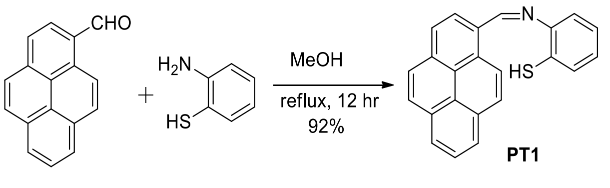

Scheme 1 Synthesis of **PT1**.

Fluorescence titrations on metal ions

Initially, **PT1** (20 μM) in DMSO/H2O (v/v = 7/3; pH 7.0) was investigated towards 60 μM (3 equiv.) of metal ions (Ag^{+}, Na^{+}, Ni^{2+}, Fe^{3+}, Co^{2+}, Zn^{2+}, Cd^{2+}, Pb^{2+}, Cr^{3+}, Mg^{2+}, Cu^{2+}, Mn^{2+}, Hg^{2+}, Fe^{2+} and Al^{3+}) in H_2O. As noticed in Fig 1a and 1b, **PT1** shows better selectivity towards Hg^{2+} ions, upon treating with 3 equiv. of metal ions and exhibited the UV-Vis and turn-on emission peaks at 365 and 445 nm with 18 nm red shift from the origin (**PT1**; λ_{abs}=347 nm and λ_{em}=427 nm; Φ = 0.041). Furthermore, the CHEF for **PT1**+Hg^{2+} was found to be 31 folds with 7 folds of quantum yield (**PT1**+Hg^{2+}; Φ = 0.289) enhancement. In addition, the above selectivity was further confirmed further by single and dual metal studies as follows. In order to establish the specific selectivity of **PT1** to Hg^{2+}, we executed the single and dual metal competitive analysis as noticed in Fig. 2. In single metal system (red bars), all the metal (Ag^{+}, Na^{+}, Ni^{2+}, Fe^{3+}, Co^{2+}, Zn^{2+}, Cd^{2+}, Pb^{2+}, Cr^{3+}, Mg^{2+}, Cu^{2+}, Mn^{2+}, Hg^{2+}, Fe^{2+} and Al^{3+}) concentrations kept as 60 μM towards **PT1**. However, for dual-metal (black bars) studies, two equal amounts of aqueous solutions of Hg^{2+} and other metal ions (60 μM + 60 μM) were combined. In addition, during dual metal analysis, 120 μM of Hg^{2+} was also considered for its effect and the obtained results demonstrated specific selectivity of **PT1** towards Hg^{2+} ions as noticed in Fig. 2. Interestingly, Pb^{2+} and Cd^{2+} ions also evidenced the little sensitivity with **PT1**, which was not enough to compete with Hg^{2+} as noticed in Figs. 1 and 2. Whereas, during dual metal studies, the presence of Pb^{2+} and Cd^{2+} ions were further enhanced the emission intensity as well. Similarly, the above metal ions were not showed any informative peaks in the UV-Vis analysis as shown in Fig 1b. The photograph of **PT1**+Hg^{2+} (visualized under UV- light irradiations) well confirmed its sensitivity by strong blue emission, as depicted in Fig. 3.

Fluorescence titrations on Hg^{2+} sensor

By increasing the concentrations of Hg^{2+} (0-60 μM with an equal span of 3 μM in H_2O) the sensitivity of **PT1** (20 μM) in DMSO/H_2O (v/v = 7/3; pH 7.0) towards Hg^{2+} ions were clearly observed in Fig. 4. The fluorescence spectrum of **PT1** (λ_{em} = 445 nm) showed turn-on responses rapidly and the inset illustrated the fluorescence intensity changes as a function of Hg^{2+} concentration. Furthermore, the CHEF and quantum yield (Φ)

values of **PT1**+Hg^{2+} sensor response increased to 31 and 7 folds, respectively, due to its strong fluorescent nature. Moreover, upon the addition of Hg^{2+} ions, the emission peak of **PT1** at 427 nm red shifted to 445 nm, which may arose from the strong Hg^{2+}-S interactions of free thiol group present in **PT1**.

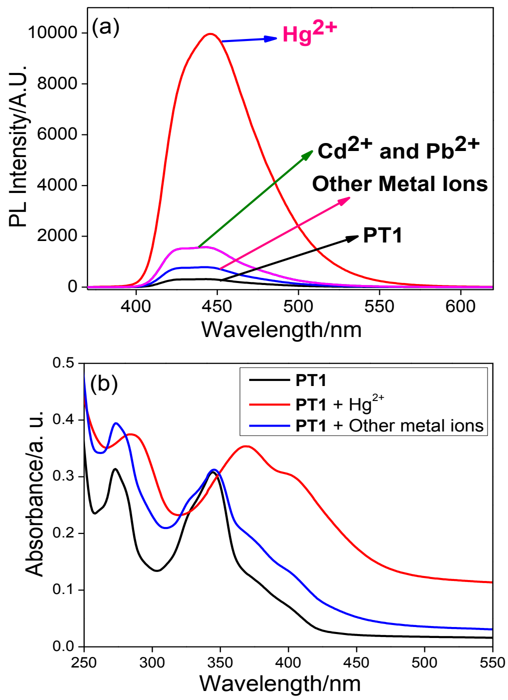

Fig. 1 Sensor response of **PT1** ($1x10^{-5}$ M) in DMSO/H2O (v/v = 7/3; pH 7.0) (λ_{ex}=347 nm) with 3 equiv. of metal ions (a) Fluorescence spectra and (b) UV-Vis spectra.

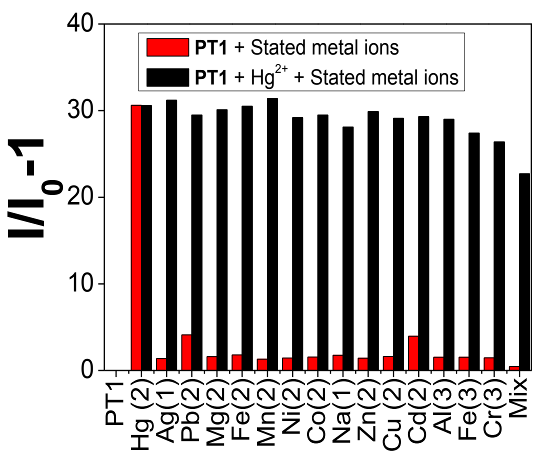

Fig. 2 Relative fluorescence intensity changes of **PT1** (20 µM) in DMSO/H_2O (v/v = 7/3; pH 7.0) (λ_{ex} = 347 nm) with 60 µM of metal ions in H_2O. Red bar; **PT1** (20 µM) in DMSO/H_2O (v/v = 7/3; pH 7.0) with 60 µM of stated metal ions in H_2O. Black bar; **PT1** (20 µM) in DMSO/H_2O (v/v = 7/3; pH 7.0) with 60 µM Hg^{2+} + 60 µM of stated metal ions in H_2O. (120 µM of Hg^{2+} was taken for Hg^{2+} effect, in dual metal analysis; Mix = Mixture of all metals except Hg^{2+}).

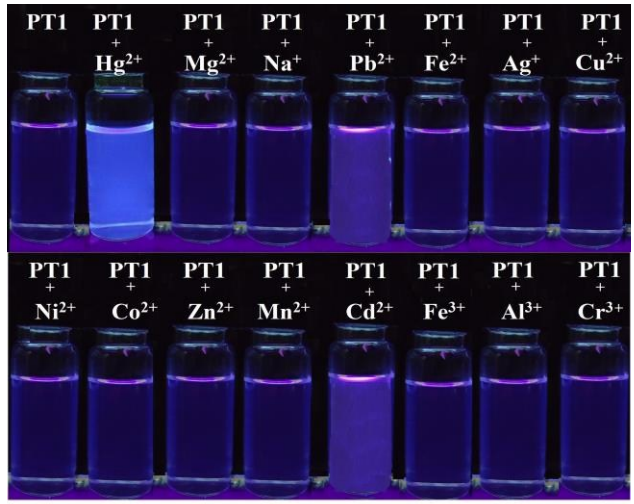

Fig. 3 Photograph of sensor selectivity of **PT1** (20 µM) in DMSO/H_2O (v/v = 7/3; pH 7.0) towards metal ions (60 µM) visualized under UV-light irradiation (λ = 365 nm).

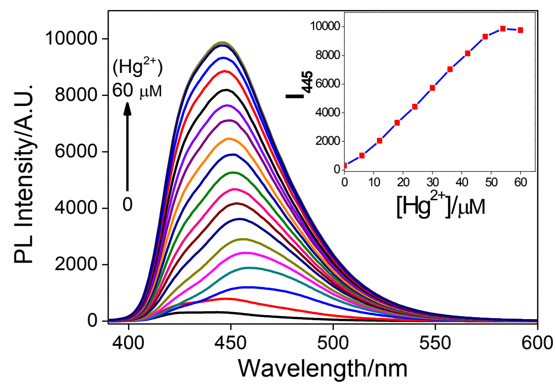

Fig. 4 Fluorescence spectra of (a) **PT1** (20 µM) in DMSO/H_2O (v/v = 7/3; pH 7.0) (λ_{ex} = 347 nm) with 0-60 µM of Hg^{2+} in H_2O (with an equal span of 3 µM). Insets: fluorescence intensity changes at 445 nm with respect to Hg^{2+} concentrations.

Stoichiometry[29] and binding sites

To ensure the binding site of sensor response of PT1, the stoichiometry of **PT1**+Hg^{2+} was calculated through job's plot as noticed in Fig. 5. The stoichiometry of **PT1**+Hg^{2+} was established by job's plots between mole fraction (X_M) and the ratio of absorption maximum changes at 365 and 347 nm (A_{365}/ A_{365}). Upon the addition of 0-42 µM of Hg^{2+} (with an equal span of 3 µM), the absorption maxima of **PT1** was quenched at 347 nm and a new peak appears at 365 nm as noticed in Fig. 5a. Therefore, the job's plots were plotted between X_M and the ratio of absorption maximum changes at 365 and 347 nm (A_{365}/ A_{347}) for **PT1**+Hg^{2+}, where it went through a maximum at molar fraction of ca. 0.405 (**PT1**+Hg^{2+}) as shown in Fig. 5b, representing the 2:1 stoichiometric complex. Similar to job's plot, the stoichiometry was further supported by ^{1}H NMR titrations[30] along with binding sites confirmation as presented in Fig. 6. In addition to stoichiometry, upon the addition of 0.5 equiv. of Hg^{2+} ions to **PT1** in d6-DMSO, the –SH peak at 7.254 ppm was completely disappeared along with upfield shift of –CH peak of –

CH=N from 7.54 ppm to 7.43 ppm without affecting the rest of the proton environment. Hence, confirmed the involvement of hetero atoms (S and N) and their chelation to form the excimer **PT1**-**PT1*** for the sensing mechanism. Furthermore, the ESI-mass peak at m/z = 875.4 [$(\textbf{PT1})_2$-Hg^{2+} +1] also supported the 2:1 sensor complex and excimer formation as noticed in Fig. S7 (ESI). Interestingly, the binding sites and the excimer mechanism was well proved by the reversibility of **PT1**+Hg^{2+} sensor complex. **PT1**+Hg^{2+} was found to be reversible to its original state (Fig. 7a), during the addition of 10 μM of disodium salt of ethylene diamine tetra-acetic acid (EDTA)[31] in H_2O and can be reusable up to 4 cycles as demonstrated in Fig. 7b. Therefore, the possible sensing mechanism based on the excimer formation was proposed based on stoichiometry, ^{1}H-NMR and ESI-Mass studies as noted in Fig 8.

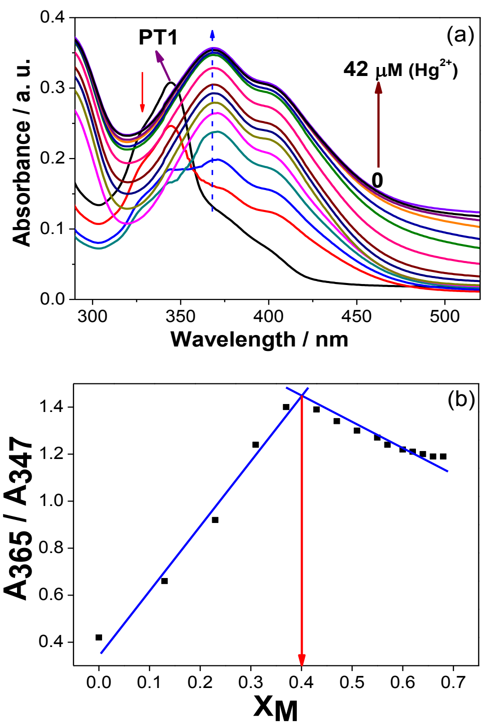

Fig. 5 Absorbance spectral changes of (a) **PT1** ($1x10^{-5}$ M) in DMSO/H_2O (v/v = 7/3; pH 7.0), titrated with 0-42 μM (with an equal span of 3 μM) of Hg^{2+} ions in H_2O and (b) stoichiometry calculation based on ratio of absorbance changes at 365 and 347 nm; $X_M = [Hg^{2+}] / [Hg^{2+}] + [\textbf{PT1}]$; where X_M = mole fraction, $[Hg^{2+}]$ and [**PT1**] are concentrations of Hg^{2+} and **PT1**; **PT1**+Hg^{2+} = 2:1 stoichiometry (ca. 0.405).

Detection limit (LOD) and association constant (K_a)

In order to prove the selectivity of **PT1** towards Hg^{2+} ions, the calculations of detection limit (LOD)[32] was performed through standard deviation and linear fittings as shown in Fig. 9a. By plotting the relative fluorescence intensity (I/I_0) changes as a function of concentration, the detection limit of **P1**+Hg^{2+} was calculated as 2.82×10^{-6} M. Assuming a 2:1 complex formation, the association constant (k_a) of **PT1**+Hg^{2+} was calculated on the basis of the following equation.[33]

$$1/(I - I_0) = 1/\{K_a \times (I_{max} - I_0) \times [Hg^{2+}]\} + 1/(I_{max} - I_0) \text{--------} 1$$

where I is the fluorescence intensity at 445 nm at any given Hg^{2+} concentration and I_0 is the fluorescence intensity at 445 nm in the absence of Hg^{2+}. The association constant K_a was evaluated graphically by plotting $1/(I - I_0)$ against $1/[Hg^{2+}]$. The typical plot $\{1/(I - I_0)$ vs. $1/[Hg^{2+}]\}$ is shown in Fig. 9b. Data were linearly fitted according to the equation (1) and the K_a value was obtained from the slope of the line.The K_a values of **PT1**+Hg^{2+} was estimated as 7.36×10^4 M^{-1}. Furthermore, to confirm the better selectivity of **PT1**, the pH and time resolved fluorescence studies were carried out as explained next.

pH and Time resolved photoluminescence spectra (TRPL)[34]

The **PT1**+Hg^{2+} sensor selectivity was verified between 3-12 pHs, maintained by the respective buffers (100 μM). In contrast to separate titrations (Fig. S4a, ESI) of pHs (3-12) solutions (100 μM) to **PT1**, the **PT1**+Hg^{2+} sensor was evidenced a better turn-on responses between pH ranges 6-8. In addition, **PT1**+Hg^{2+} sensor was also notified the incredible response at pHs 9 and 10. But, considering the folds of emission enhancement, only 6-8 pHs are suitable for **PT1**+Hg^{2+} sensor selectivity. Similar to pH studies, the TRPL decay constants (τ) was affected typically by turn-on sensor response as summarized in Tables 1 and S1 (ESI). From the TRPL signals (Fig. S4b, ESI) without any sensor response the fluorescence life time value of **PT1** was about 2.63 ns. Whereas, during the **PT1**+Hg^{2+} sensing process, the faster decay component (A_1) of **PT1** (32.78%) was increased to 94.46%, along with decreased values of longer decay component (A_2) from 67.22 to 5.54% as shown in Table S1(ESI). Based on single exponential decay fitting, the average fluorescence life time value of **PT1**+ Hg^{2+} was estimated as 3.14 ns. The decay constant (τ) values of **PT1**+ Hg^{2+} and **PT1**+ Hg^{2+} + EDTA, supported the off-on-off reversible etiquette formation along with CHEF and excimer formation.

Counter ion effect on sensor response[35]

Since many sensor responses were affected by the presence of counter ions, we performed the sensor titrations of **PT1** towards Hg^{2+} with different counter ions (CH_3COO^-, NO_3^-, Cl^-, I^-, ClO_4^- and SO_4^{2-}). As evidenced in Fig S8 (ESI), the CHEF of Hg^{2+} sensor response was found in-between 27 to 30 folds. However, the sensor response in the presence of acetate (CH_3COO^-) and nitrate (NO_3^-) were evidenced the similar CHEF (30 folds) enhancement. On the other hand, the presence of sulphate (SO_4^{2-}) evidenced the slight decrease in the CHEF (27 folds) among other ions; but, it was not enough to affect the sensor selectivity. Similarly, other counter ions such as Cl^-, I^-, ClO_4^- were also not affect the Hg^{2+} sensor response extremely. Hence, it was concluded that Hg^{2+} sensor response of **PT1** was not affected incredibly in the presence of different counter ions.

Computational analysis[28,36]

To elucidate the structures of **PT1** and **PT1**+Hg^{2+} complexes, density functional theory (DFT) calculations were undertaken using the Gaussian 09 software package. Chemosensor **PT1** and

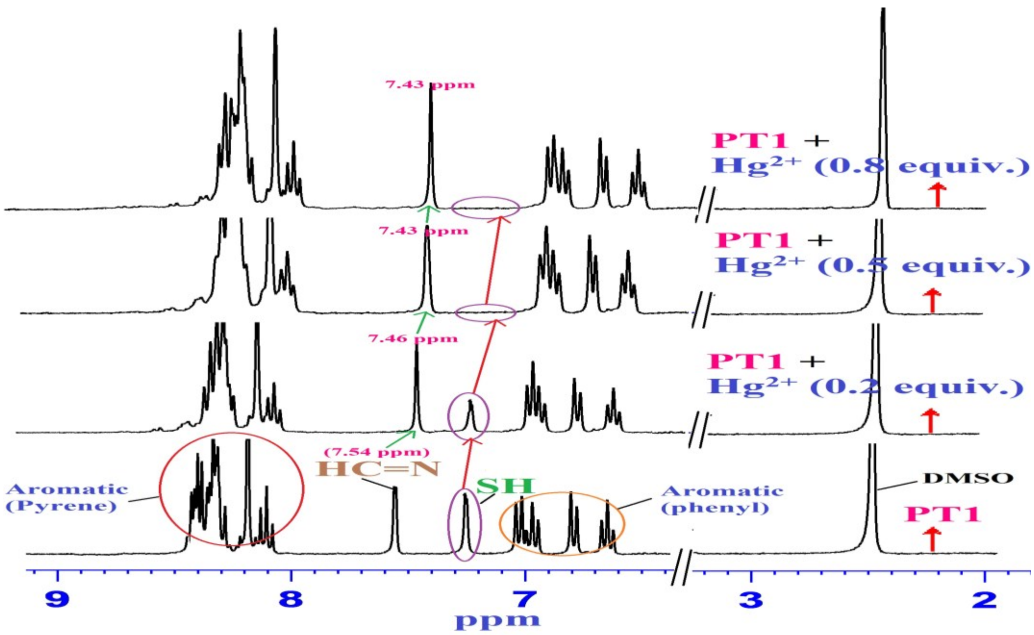

Fig. 6 [1]H NMR spectral changes of **PT1** (20 mM) in d6-DMSO with 0 - 16 mM of Hg^{2+} in D_2O.

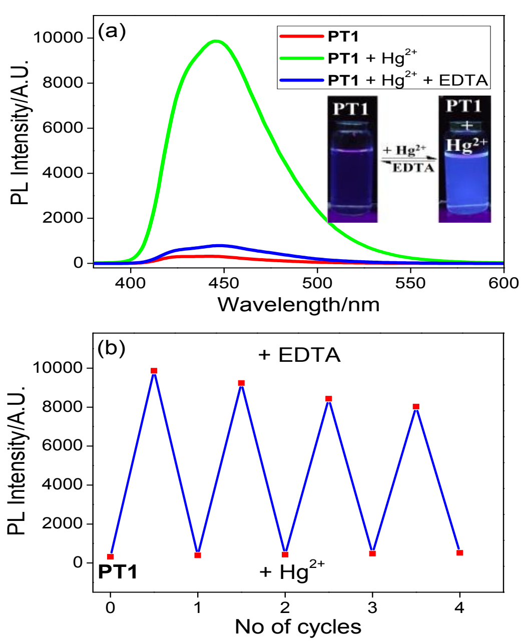

Fig. 7 (a) Sensor reversibility and (b) Reversible cycles of **PT1** + Hg^{2+} with EDTA.

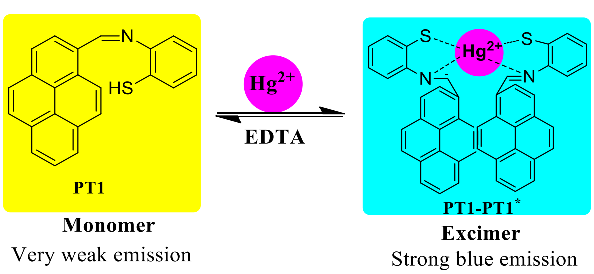

Fig. 8 Possible proposed binding mechanism of **PT1** towards Hg^{2+} ions.

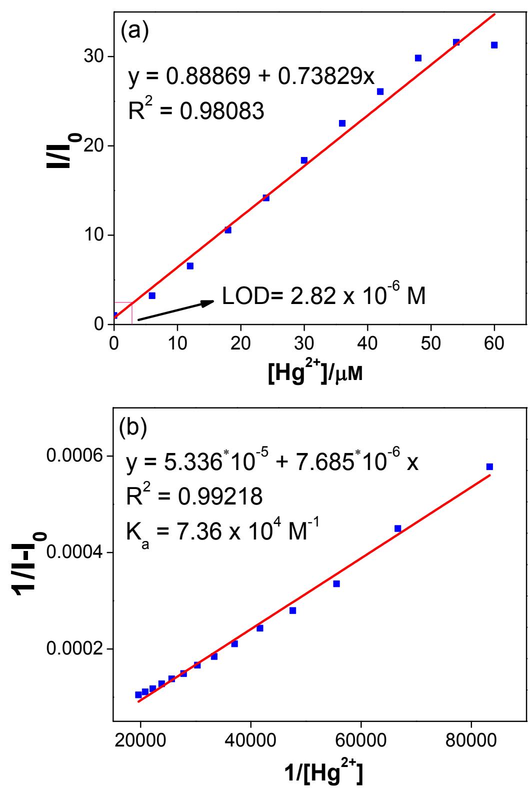

Fig. 9 (a) Standard deviation and linear fittings for detection limit calculations of **PT1** + Hg^{2+} based on relative fluorescence intensity changes versus Hg^{2+} metal ion concentrations and (b) Benesi–Hildebrand plot of **PT1** with Hg^{2+} in DMSO/H_2O (v/v = 7/3; pH 7.0). The excitation wavelength was 347 nm and the observed wavelength was 445 nm. The binding constant was 7.36 x 10^4 M^{-1} for Hg^{2+} binding with **PT1**.

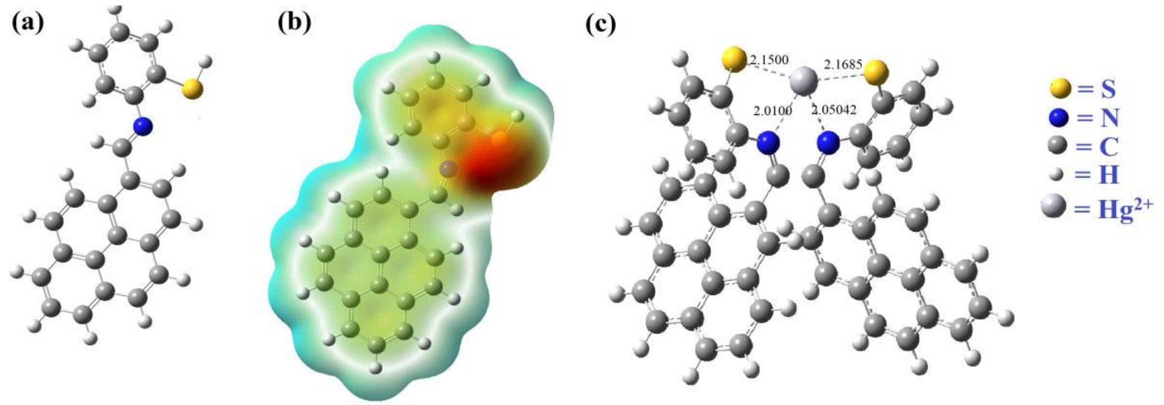

Fig. 10 (a) DFT optimized structure of **PT1**, (b) Molecular electrostatic potential (MEP) of **PT1** and (c) optimized structure of **PT1**+Hg^{2+} in gas phase.

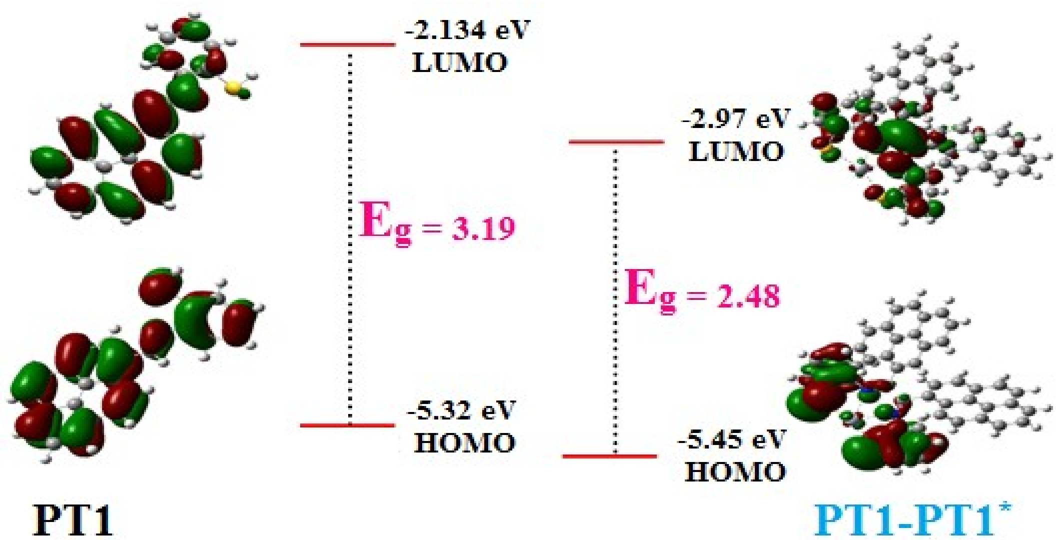

Fig. 11 HOMOs, LUMOs and band gaps of **PT1** and **PT1**+Hg^{2+} (**PT1-PT1***) complexes.

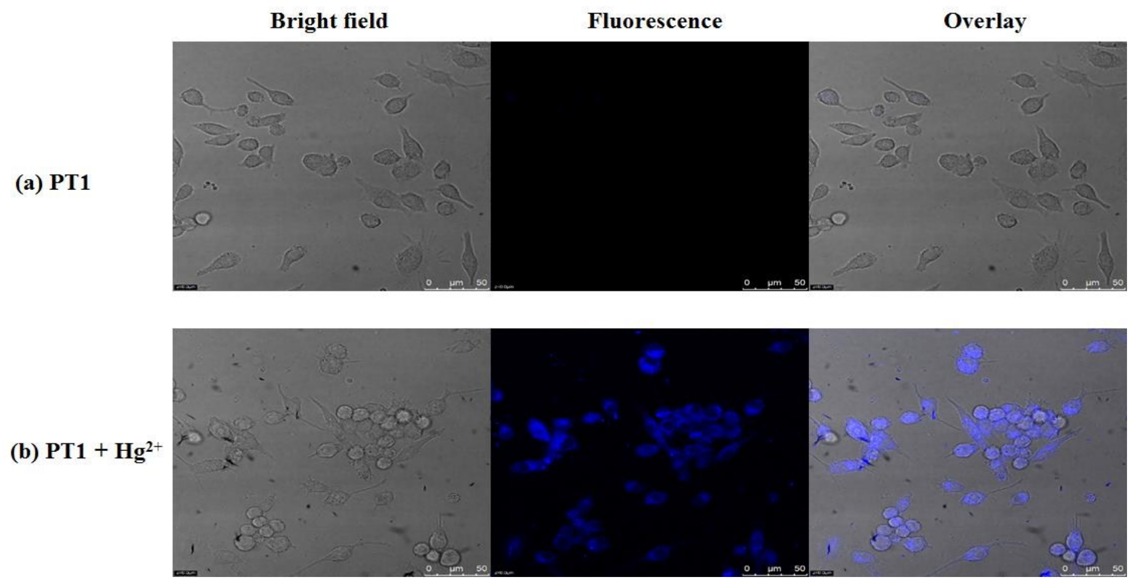

Fig. 12 Fluorescence images of Hela cells treated with **PT1** and Hg^{2+}. Bright Field image (Left); Fluorescence image (middle); Merged image (right). The scale bar is 50 μM.

PT1+Hg^{2+} complexes were subjected to energy optimization by using B3LYP/6-31G (D) and B3LYP/LANL2DZ, respectively. Fig. 10 revealed the optimized structure of **PT1** at B3LYP/6-31G (D) (with molecular electrostatic potential) and **PT1**+Hg^{2+} complex at B3LYP/LANL2DZ in gas phase. The distances of Hg^{2+} from the two S atoms are about 2.1685 Å and 2.1500 Å. Similarly, the distances of Hg^{2+} from the two N atoms are around 2.05042 Å and 2.0100 Å. Notably, the HOMO-LUMO energy gaps obtained from DFT studies also well supported the excimer formation mechanism. In addition, the bandgap between HOMO (-5.32 eV) and LUMO (-2.13 eV) of **PT1** was calculated as 3.19 eV. On the other hand, due to the formation of excimer (**PT1-PT1***) via **PT1**+Hg^{2+} coordination, the bandgap between the HOMO (-5.45 eV) and LUMO (-2.97 eV) was further decreased to 2.48 eV. In Table 1, the DFT properties such as HOMO, LUMO and their energy gaps (HLP) are presented.

Attributed to the importance of DFT studies, our further evaluation illustrated that apart from bandgap, the electron density of **PT1** was distributed throughout the structure as noted in Fig. 11. However, upon chelation to Hg^{2+}, the formed excimer (**PT1**-**PT1***) evidenced the electron density located on **PT1**+Hg^{2+} complex. The above observations influence the electron transfer and emission intensity of **PT1** towards Hg^{2+} ions. Hence, Fluorescent turn-on sensor response for Hg^{2+} ions detection was witnessed. Furthermore, as illustrated in Fig. S5, the electron clouds of HOMOs and LUMOs (HOMO, HOMO-1 and LUMO, LUMO+1) in **PT1** were located on all over the molecule. Meanwhile, except LUMO+1 they were positioned towards **PT1**+Hg^{2+} complex in **PT1**-**PT1*** as noticed in Fig. S6. Hence, confirmed the **PT1**-**PT1*** excimer formation and CHEF induced emission enhancement of **PT1** with Hg^{2+} ions.

Living cell imaging

The potential of **PT1** for imaging of Hg^{2+} in living cells were obtained using a confocal fluorescence microscope. When Hela cells were incubated with **PT1** (20 μM), no fluorescence was observed (Fig. 12a). After the treatment with Hg^{2+}, a bright blue fluorescence was observed in the Hela cells (Fig. 12b). An overlay of fluorescence and bright-field images shows that the fluorescence signals are localized in the intracellular area, indicating a subcellular distribution of Hg^{2+} and good cell-membrane permeability of **PT1**.

Conclusions

In conclusion, novel pyrene based free thiol containing schiff base derivative **PT1** was synthesized via one-pot reaction and utilized as Hg^{2+} turn-on sensor. The 2:1 stoichiometry of sensor complexes **PT1**+Hg^{2+} was calculated from job plot based on UV-Vis absorption titrations. In addition, the binding sites of sensor complex **PT1**+Hg^{2+} was well established from ^{1}H NMR titrations and supported by the ESI-mass analysis and off-on-off reversible etiquette formation of **PT1**+Hg^{2+} via successive addition of Hg^{2+} and EDTA, respectively, up to 4 cycles. Hence, the possible sensing mechanism through excimer (**PT1-PT1***) formation was proposed. Furthermore, by standard deviation and linear fittings the detection limit (LOD) of **PT1**+Hg^{2+} was calculated as 2.82 x 10^{-6} M. Similarly, based on Benesi-Hildebrand plot the association constant (Ka) of **PT1**+Hg^{2+} was estimated as 7.36 x 10^4 M^{-1}. More importantly, the DFT calculation supported the sensor selectivity by the decrease in the energy gap between HOMO and LUMO. In addition, **PT1** sensor selectivity was well supported by TRPL studies, pH effect and quantum yield calculations and applied for the detection of Hg^{2+} in living cells.

Experimental

Materials and methods

General Information

All anhydrous reactions were carried out by standard procedures under nitrogen atmosphere to avoid moisture. The solvents were dried by distillation over appropriate drying agents and reactions were monitored by TLC plates. ^{1}H and ^{13}C NMR were recorded on a 300 MHz Bruker spectrometer. The chemical shifts (δ) are reported in ppm and coupling constants (*J*) in Hz and relative to TMS (0.00) for ^{1}H and ^{13}C NMR, (s, d, t, q, m, and dd means single, double, ternary, quadruple, multiple, and doublet of doublet, respectively), and d-chloroform [at 7.26 ppm (^{1}H NMR) & 77.0 ppm (^{13}C NMR)] and d6-DMSO (at 2.49 ppm) for ^{1}H NMR titrations were used as references. Mass spectra (FAB and ESI) were obtained on the respective mass spectrometer. Absorption and fluorescence spectra were measured on JASCO V-650 Spectrophotometer and F-4500 Fluorescence Spectrophotometer, respectively. Identification and purity of the compound **PT1** was characterized by NMR (^{1}H & ^{13}C), and Mass (FAB). The time-resolved photoluminescence (TRPL) spectra were measured using a home-built single photon counting system. Excitation was performed using a 440 nm diode laser (Picoquant PDL-200, 50 ps fwhm, 2 MHz). The signals collected at the excitonic emissions of solutions were connected to a time-correlated single photon counting card (TCSPC, Picoquant Timeharp 200). The emission decay data were analyzed with the biexponential kinetics in which two decay components were derived. The lifetime values (τ_1 and τ_2) and pre-exponential factors (A_1 and A_2) were determined and summarized. 3-12 pH buffers were freshly prepared as per the literature.[37] Fluorescence microscopic images were taken using Leica TCS SP2 Confocal Fluorescence Microscope.

Sensor titrations

Compound **PT1** was dissolved in DMSO/H_2O (7/3) and Na^+, Ni^{2+}, Fe^{3+}, Cd^{2+}, Cr^{3+}, Mg^{2+}, Cu^{2+}, Fe^{2+} and Al^{3+} metal cations were dissolved in water medium at 1x10^{-4} M concentration from their respective chloro compounds. Similarly, Ag^+, Co^{2+}, Zn^{2+}, Pb^{2+}, Mn^{2+}, and Hg^{2+} metal cations were dissolved in water medium at 1x10^{-4} M concentration from their respective acetate salts. Disodium salt of ethylene diamine tetra acetic acid (**EDTA** at 1x10^{-4} M) was dissolved in H_2O for sensor reversibility.

procedure[27] for the synthesis of compound PT1

To 1 equiv. of 2-amino thiophenol in 50 ml of methanol, 1 equiv. of Pyrene-1-carboxaldehyde was added with constant stirring under nitrogen and then refluxed for 12 hrs. The reaction was monitored by TLC, after completion, the reaction mixture was cooled and the solvent was evaporated to give the crude product, which was recrystallized from ethanol to afford pure compound as yellow powder.

2-((pyren-1-ylmethylene)amino)benzenethiol (**PT1**): Bright yellow powder; 92% yield; ^{1}H NMR (300 MHz, $CDCl_3$) δ: 4.58 (s, 1H (-SH)), 6.62 – 6.80 (m, 2H), 6.95 – 7.04 (m, 2H), 7.56 (s, 1H (-CH=N)), 8.08 – 8.42 (m, 9H); ^{13}C NMR (75 MHz, $CDCl_3$) δ: 115.04, 115.96, 120.20, 121.63, 123.41, 125.77, 125.95, 126.03, 127.19, 128.53, 129.28, 133.41, 136.56, 156.38, 160.20; FAB: calculated: m/z = 337 (M^+, 100%); Found: m/z = 337 (M^+, 100%).

Procedure for fluorescence imaging

PT1 was also applied to living cell imaging. For the detection of Hg^{2+} in living cells, HeLa cells were cultured in DMEM (Dulbecco's Modified Eagle's Medium, high glucose) supplemented with 10% FBS at 37°C and 5% CO_2. Cells were plated on 14mm glass coverslips and allowed to adhere for 24hours.

The cell image was performed in PBS with 10µm Hg $(OAc)_2$. The cells cultured in DMEM were treated with of 10µm Hg^{2+} dissolved in sterilized PBS (pH7.4) and incubate for 30 min at 37^0C and then wash the treated cells for three times with 2 ml PBS to remove the remaining metal ions. Add 2ml of culture media to the cell culture and treat the cell culture with 20µm of **PT1** dissolved in DMSO followed by incubate (60 min at 37^0C). The culture medium was removed, and the treated cells were washed with PBS (2ml) before observation. Fluorescence imaging was formed with a Leica TCS SP2 Confocal fluorescence microscope. The cells were excited with a white light laser at λ_{ex} = 347 nm at 6% output and collecting emission between 430 ± 495 nm (**PT1**+Hg^{2+}).

Computational methods

Quantum chemical calculations based on density functional theory (DFT) were carried out using a Gaussian 09 program. The ground-state structures of **PT1** and the **PT1**+Hg^{2+} complexes were computed using the density functional theory (DFT) method with the hybrid-generalized gradient approximation (HGGA) functional B3LYP. The 6-31G basis set was assigned to nonmetal elements (C, H, N and S). For the **PT1**+Hg^{2+} complex, the LANL2DZ basis set was used for Hg^{2+}, whereas the 6-31G basis set was used for other atoms.

Acknowledgment

This work was supported by the International Research Center of Kalasalingam University (IRC-KLU), Krishnan Koil 626 190, India. Further, KLU is grateful to authors Y. C. Rajan and P. Balu for their valuable contributions in TRPL, live cell imaging and DFT studies.

Notes and references

† Electronic Supplementary Information (ESI) available for ^{1}H, ^{13}C NMR and mass (FAB); pH effect, TRPL data and DFT images of sensor complexes. See DOI: 10.1039/b000000x/

1 (a) V. Amendola, L. Fabbrizzi, F. Forti, M. Licchelli, C. Mangano, P. Pallavicini, A. Poggi, D. Sacchi and A. Taglieti, *Coord. Chem. Rev*., 2006, **250**, 273; (b) D. Astruc, E. Boisselier and C. Ornelas, *Chem. Rev*. 2010, **110**, 1857.

2 (a) Y. Yang, Q. Zhao, W. Feng and F. Li, *Chem. rev*., 2012, **113**,192; (b) K. Kaur, R. Saini, A. Kumar, V. Luxami, N. Kaur, P. Singh and S. Kumar, *Coord. Chem. Rev*., 2012, 256, 1992.

3 (a) S. Pal, N. Chatterjee and P. K. Bharadwaj, *Chem. Soc. Rev*., 2014, **4**, 26585; (b) H. Zhu, J. Fan, B. Wang and X. Peng, *Chem. Soc. Rev*., 2015, DOI: 10.1039/C4CS00285G; (c) M. Sarkar, S. Banthia, A. Patil, M. B. Ansari and A. Samanta, *New J. Chem*., 2006, **30**, 1557; (d) R. Hu, L. Zhang and H. Li, *New J. Chem*., 2014, **38**, 2237.

4 . (a) F. D. Natale, A. Lancia, A. Molino, M. D. Natale, D. Karatza and D. Musmarra, *J. Hazard. Mater*., 2006, **132**, 220; (b) P. B. Tchounwou, W. K. Ayensu, N. Ninashvili and D. Sutton, *Environ. Toxicol*. 2003, **18**, 149; (c) R. Eisler, *Environ. Geochem. Health*., 2003, **25**, 325; (d) I. Onyido, A. R. Norris and E. Buncel, *Chem. Rev*. 2004, **104**, 5911.

5. (a) T. W. Clarkson, L. Magos and G. J. Myers, *New Engl. J. Med*. 2003, **349**, 1731; (b) M. Harada, *Crit. Rev. Toxicol*., 1995, **25**, 1; (c) B. Liu, F. Zeng, Y. Liu and S. Wu, *Analyst*, 2012, **137**, 1698.

6. (a) C. M. L. Carvalho, E. H. Chew, S. I. Hashemy, J. Lu and A. Holmgren, *J. Biol. Chem*. 2008, **283**, 11913; (b) Z. Guo, J. Duan, F. Yang, M. Li, T. Hao, S. Wang and D. Wei, *Talanta* 2012, **93**, 49; (c) J. Hu, J. Li, J. Qi and J. Chen, *New J. Chem*., 2015, DOI: 10.1039/C4NJ01147C.

7. (a) W. F. Fitzgerald, C. H. Lamborg and C. R. Hammerschmidt, *Chem. Rev*., 2007, **107**, 641; (b) M. H. Keefe, K. D. Benkstein and J. T. Hupp, *Coord. Chem. Rev*., 2000, **205**, 201; (c) P. B. Tchounwou, W. K. Ayensu, N. Ninashvili and D. Sutton, *Environ. Toxicol*., 2003, **18**, 149; (d) C. N. Glover, D. Zheng, S. Jayashankar, G. D. Sales, C. Hogstrand and A.-K. Lundebye, *Toxicol. Sci*., 2009, **110**, 389; (e) M. Korbas, S. R. Blechinger, P. H. Krone, I. J. Pickering and G. N. George, *Proc. Natl. Acad. Sci. U. S. A*., 2008, **105**, 12108.

8. (a) A. P. de Silva, H. Q. N. Gunaratne, T. Gunnlaugsson, A. J. M. Huxley, C. P. McCoy, J. T. Rademacher and T. E. Rice, *Chem. Rev*., 1997, **97**, 1515; (b) A. K. Dwivedi, G. Saikia and P. K. Iyer, *J. Mater. Chem*., 2011, **21**, 2502.

9. (a) Z. Yang, J. Cao, Y. He, J. H. Yang, T. Kim, X. Peng and J. S. Kim, *Chem. Soc. Rev*., 2014, **43**, 4563; (b) X. Qian, Y. Xiao, Y. Xu, X. Guo, J. Qian and W. Zhu, *Chem. Commun*., 2010, **46**, 6418.

10. (a) J. Yin, Y. Hu and J. Yoon, *Chem. Soc. Rev*., 2015, DOI: 10.1039/C4CS00275J; (b) L. Zhang, H. Huang, N. Xu and Q. Yin, *J. Mater. Chem. B*, 2014, **2**, 4935; (c) W. Wang, Q. Wen, Y. Zhang, X. Fei, Y. Li, Q. Yang and X. Xu, *Dalton Trans*., 2013, **42**, 1827.

11. (a) N. Niamnont, R. Mungkarndee, I. Techakriengkrai, P. Rashatasakhon and M. Sukwattanasinitt, *Biosensor and Bioelectronics*, 2010, **26**, 863; (b) X. Lou, D. Ou, Q. Li and Z. Li, *Chem. Commun*., 2012, **48**, 8462.

12. (a) D. T. McQuade, A. E. Pullen and T. M. Swager, *Chem. Rev*., 2000, **100**, 2537; (b) G. Aragay, J. Pons and A. Merkoci, *Chem. Rev.*, 2011, **111**, 3433.

13. (a) M. Sauer, *Angew. Chem. Int. Ed*., 2003, **42**, 1790; (b) M. Shamsipura, T. Poursaberib, M. Hassanisadib, M. Rezapour, F. Nourmohammadianc and K. Alizadeh, *Sensors and Actuators B*, 2012, **161,** 1080; (c) M. Formica, V. Fusi, L. Giorgi and M. Micheloni, *Coord. Chem. Rev*., 2012, **256**, 170.

14. (a) K. Hanaoka, Y. Muramatsu, Y. Urano, T. Terai and T. Nagano, *Chem. Eur. J*., 2010, **16**, 568; (b) Y. Chen, C. Zhu, Z. Yang, J. Li, Y. Chiao, W. He, J. Chen and Z. Guo, *Chem. Commun*., 2012, **48**, 5094;

15. (a) D. A. Pearce, N. Jotterand, I. S. Carrico and B. Imperiali, *J. Am. Chem. Soc*., 2001, **123**, 5160; (b) M. Mameli, M. C. Aragoni, M. Arca, C. Caltagirone, F. Demartin, G. Farruggia, G. D. Filippo, F. A. Devillanova, A. Garau, F. Isaia, V. Lippolis, S. Murgia, L. Prodi, A. Pintus and N. Zaccheroni, *Chem. Eur. J*., 2010, **16**, 919; (c) Y. Bao, B. Liu, F. Du, J. Tian, H. Wang and R. Bai, *J. Mater. Chem*., 2012, **22**, 5291.

16. (a) L. Fabbrizzi, M. Licchelli, F. Mancin, M. Pizzeghello, G. Rabaioli, A. Taglietti, P. Tecilla and U. Tonellato, *Chem. Eur. J*., 2002, **8**, 94; (b) Y. Ni and J. Wu, *Org. Biomol. Chem*., 2014, **12**, 3774.

17. (a) R. R. Crichton, A. Florence and R. J. Ward, *Coord. Chem. Rev*., 2002, **228**, 365; (b) S. Muthaiah, Y. C. Rajan, and H. C. Lin, *J. Mater. Chem*., 2012, **22**, 8976.
18. C. Ma, A. Lo, A. Abdolmaleki and M. J. MacLachlan, *Org. Lett*., 2004, **6**, 3841; (b) J. Du, M. Hu, J. Fan and X. Peng, *Chem. Soc. Rev*., 2012, **41**, 4511.
19. (a) J. A. Drewrya and P. T. Gunninga, *Coord. Chem. Rev*., 2011, **255**, 459; (b) S. Muthaiah, M. V. R. Raju, H. C. Lin, K. H. Wei and H. C. Lin, *J. Mater. Chem.* A, 2014, **2**, 17463.
20. (a) D. Maity, A. K. Manna, D. Karthigeyan, T. K. Kundu, S. K. Pati and T. Govindaraju, *Chem. Eur. J*., 2011, **17**, 11152; (b) D. Maity and T. Govindaraju, *Inorg. Chem*. 2011, **50**, 11282; (c) J. F. Jang, Y. Zhou, J. Yoon and J. S. Kim, *Chem. Soc. Rev*., 2011, **40**, 3416. (d) S. Muthaiah, Y. H. Wu and H. C. Lin, *Analyst*, 2013, **138**, 2931; (e) S. Muthaiah, Y. H. Wu, A. Singh, M. V. R. Raju and H. C. Lin, *J. Mater. Chem.* A, 2013, **1**, 1310. (f) A. Singh, R. Singh, S. Muthaiah, E. C. Prakash, H. C. Chang, P. Raghunath, M. C. Lin and H. C. Lin, *Sens. And Acut. B*, 2015, **207**, 338.
21. (a) S. Karupannan and J. C. Chambron, *Chem. Asian. J*. 2011, **6**, 964 and references therein. (b) L. Fabbrizzi, M. Lichelli, P. Pallavicini, D. Sacci and E. Taglietti, *Analyst*., 1996, **121**, 1763.
22. (a) M. Kumar, R. Kumar and V. Bhalla, *Org. Lett*., 2011, **13**, 366; (b) S. Sarkar, S. Roy, A. Sikdar, R. N. Saha and S. S. Panja, *Analyst*, 2013, **138**, 7119; (c) L. E. Santos-Figueroa, M. E. Moragues, E. Climent, A. Agostini, R. M. -Máñez and F. Sancenón, *Chem. Soc. Rev*., 2013, **42**, 3489.
23. (a) (c) H. P. Fang, S. Muthaiah, A. Singh, M. V. R. Raju, Y. H. Wu and H. C. Lin, *Sens. And Acut. B*, 2014, **194**, 229; (b) Y. B. Ruan, A. F. Li, J. S. Zhao, J. S. Shen, and Y. B. Jiang, *Chem. Commun*., 2010, **46**, 4938; (c) F. Miao, J. Zhan, Z. Zou, D. Tian and H. Li, *Tetrahedron*, 2012, **68**, 2409.
24. (a) F. Qu, J. Liu, H. Yan, L. Peng and H. Li, *Tetrahedron Lett*., 2008, **49**, 7438; (b) P. Mahato, S. Saha, P. Das, H. Agarwalla and A. Das, : *RSC Adv*., 2014, **4**, 36140; (c) G. Sivaraman, T. Anand and D. Chellappa, *RSC Adv*., 2012, **2**, 10605.
25. (a) Z. Yan, M. –F. Yuen, L. Hu, P. Suna and C. –S. Lee, *RSC Adv*., 2014, **4**, 48373; (b) T. Anand, G. Sivaraman, P. Anandh, D. Chellappa and S.Govindarajan, *Tetrahedron Lett*., 2014, **55**, 671; (c) Y. Lu, S. Huang, Y. Liu, S. He, L. Zhao, and X. Zeng, *Org. Lett*., 2011, **13**, 5274.
26. (a) E. M. Nolan and S. J. Lippard, *J. Am. Chem. Soc*., 2007, **129**, 5910; (b) A. Banerjee, D. Karak, A. Sahana, S. Guha, S. Lohar and D. Das, *J. Hazard. Mater*., 2011, **186**, 738; (c) M. J. Culzoni, A. M. de la pena, A. Machuca, H. C. Goicoechea and R. Babiano, *Anal. Methods*, 2013, **5**, 30.
27. (a) K. Krzysztof, and K. Biernacka, *Struct. Chem*., 2010, **21**, 357; (b) C. G. Freiherr von Richthofen, A. Stammler, H. Bogge and T. Glaser, *J. Org. Chem*., 2012, **77**, 1435.
28. C. –Y. Chou, S. –R. Liu and S. –P. Wu, *Analyst*, 2013, **138**, 3264.
29. (a) Y. Q. Weng, F. Yue, Y. R. Zhong and B. H. Ye, *Inorg. Chem*., 2007, **46,** 7749; (b) X. He, N. Zhu, and V. W. W. Yam, *Organometallics*, 2009, **28**, 3621; (c) M. H. Yang, C. R. Lohani, H. Cho and K. H. Lee, *Org. Biomol. Chem*., 2011, **9**, 2350.
30. (a) P. N. W. Baxter, *Chem. Eur. J*., 2003, **9**, 2531 – 2541; (b) W. Zhou, Y. Li, Y. Li, H. Liu, S. Wang, C. Li, M. Yuan, X. Liu, and D. Zhu, *Chem. Asian. J.* 2006, ***1-2***, 224-230.
31. (a) N. Niamnont, N. Kimpitak, K. Wongravee, P. Rashatasakhon, K. K. Baldridge, J. S. Siegel and M. Sukwattanasinitt, *Chem. Commun*., 2013,**49**, 780; (b) S. Sirilaksanapong, M. Sukwattanasinitt and P. Rashatasakhon, *Chem. Commun*., 2012, **48**, 293. (c) N. Niamnont, W. Siripornnoppakhun, P. Rashatasakhon and M. Sukwattanasinitt, *Org. Lett*., 2009, **11**, 2768.
32. J. Li, Y. Wu, F. Song, G. Wei, Y. Cheng, and C. Zhu, *J. Mater. Chem*., 2012, **22**, 478.
33. (a) H. A. Benesi and J. H. Hildebrand, *J. Am. Chem. Soc*., 1949, **71**, 2703; (b) S. Das, A. Sahana, A. Banerjee, S. Lohar, D. A. Safin, M. G. Babashkina, M. Bolte, Y. Garcia, I. Hauli, S. K. Mukhopadhyay and D. Das, *Dalton Trans*., 2013, **42**, 4757; (c) K. Tayade, S. K. Sahoo, B. Bondhopadhyay, V. K. Bhardwaj, N. Singh, A. Basu, R. Bendre and A. Kuwar, *Biosensor and Bioelectronics*, 2014, **61**, 429; (d) S. Madhu, D. K. Sharma, S. K. Basu, S. Jadhav, A. Chowdhury and M. Ravikanth, *Inorg. Chem*., 2013, **52,** 11136.
34. (a) K. Cammann, U. Lemke, A. Rohen, J. Sander, H. Wilken and B. Winter, *Angew. Chem. Int. Ed. Engl*., 1991, **30**, 516; (b) M. H. Ha-Thi, M. Penhoat, D. Drouin, M. Blanchard-Desce, V. Michelet and I. Leray, *Chem. Eur. J.*, 2008, **14**, 5941; (c) M. Schaferling, *Angew. Chem. Int. Ed*., 2012, **51**, 3532.
35. K. J. Albert, N. S. Lewis, C. L. Schauer, G. A. Sotzing, S. E. Stitzel, T. P. Vaid and D. R. Walt, *Chem. Rev*., 2000**, 100**, 2595.
36. (a) M. R. Silva-Junior and W. J. Thiel, *Chem. Theory Comput.*, 2010, **6**, 1546; (b) P. Balu, S. Baskaran, V. Kannappan and C. Sivasankar, *New J. Chem*., 2012, **36**, 562.
37. R. A. Robinson, and R. H. Stokes, *Electrolyte solutions" 2nd ed., rev.*, 1968, London, Butterworths.

Table of Contents (TOC)/ABSTRACT Graphic

A novel pyrene based free thiol containing schiff base derivative **PT1** was synthesized and reported as fluorescent turn-on sensor for Hg^{2+} ions, via CHEF and excimer (**PT1-PT1***) formation with live cell imaging.